Content list available at BioEnv

Bioresources and Environment

Journal homepage: www.bioenvuitm.com

Green Biosynthesized Silver Nanoparticles using *Ficus deltoidea* Leaf Extract as Antibacterial Agent

Ibrahirul Qamil Ismail[1], Nik Ahmad Nizam Nik Malek[1,2]*, Nor Suriani Sani[3], Shahrulnizahana Mohammad Din[4], Muhammad Hariz Asraf[1]

[1]Department of Biosciences, Faculty of Science, Universiti Teknologi Malaysia, 81310 UTM, Skudai, Johor, Malaysia.
[2]Centre for Sustainable Nanomaterials, Ibnu Sina Institute for Scientific and Industrial Research (ISI-ISIR), Universiti Teknologi Malaysia, 81310 UTM, Skudai, Johor, Malaysia.
[3]Department of Deputy Vice-Chancellor (Research and Innovation), Universiti Teknologi Malaysia, 81310 UTM Skudai, Johor, Malaysia.
[4]Department of Chemistry, Johor Branch, Jalan Abdul Samad, 80100 Johor Bahru, Johor, Malaysia.

Received July 18, 2023. Accepted in revised form September 08, 2023
Available online October 30, 2023

ABSTRACT. Hazardous and harmful reducing agents are often utilized in the silver nanoparticle (AgNP) synthesis method. Hence, various bioresources acting as reducing agents are being researched for a greener and safer AgNP synthesis. This study aimed to investigate the green synthesis of AgNP using local *Ficus deltoidea* (Mas Cotek) plant leaf extract. The plant leaf extract was analyzed for its total phenolic (TPC) and flavonoid contents (TFC), and the values were determined to be 24.37 ± 0.57 mg/g and 1118.91 ± 8.55 mg/g, respectively. The optimized values of the AgNP synthesis obtained were 0.6 ml *F. deltoidea* extract (5%) at pH 8 with the synthesis temperature at 80°C and 24 hours reaction period. The biosynthesized AgNP was characterized using UV-visible spectroscopy, showing a peak at around 440 nm to 450 nm. The Fourier transform infrared (FTIR) spectra of the AgNP and plant extract showed prominent peaks around 3400 cm^{-1}, 1600 cm^{-1}, and 1360 cm^{-1}, corresponding to the functional groups in the plant extract. Transmission electron microscope (TEM) image showed that the AgNP was spherical, with sizes ranging from 10 nm to 50 nm. Antibacterial assays that were done based on disc diffusion technique (DDT) against Gram-positive (*Staphylococcus aureus* ATCC 6538), Gram-negative (*Escherichia coli* ATCC 11229), and anaerobic skin bacterium, *Cutibacterium acnes* ATCC 6919 present significant halo-zone formation. The biocompatibility of the sample against HSF1184 human fibroblast skin cells showed that the IC_{50} value of the biosynthesized AgNP (0.25 mg/ml) was lower than the commercial AgNP (1.0 mg/ml). This study showed that the phenolic and flavonoid contents in *F. deltoidea* leaf extract enable the synthesis of AgNP and exhibit antibacterial effects against Gram-positive, Gram-negative, and skin bacteria while presenting a mild cytotoxicity level against human fibroblast cells.

Keywords: Antibacterial, Ficus deltoidea, Green synthesis, Silver nanoparticles

INTRODUCTION

In general, conventional synthesis of silver nanoparticles (AgNP) involves physical and chemical methods. The physical methods relied upon several techniques, such as ball milling process, evaporation-condensation process, arc discharge process, laser ablation process, and spray pyrolysis process (Kaabipour and Hemmati, 2021). These methods, however, are generally expensive and require high amounts of energy coupled with complex tools and equipment. In addition, technical disadvantages posed by these methods influence the scale-up production of AgNP to obtain in bulk quantities. One example is the laser ablation method, where a high-energy laser beam is used to

*Corresponding author: Tel.: +60137805466.
E-mail address: *niknizam@utm.my*

ablate metallic silver and confine it in the surrounding ambient (Verma et al., 2017). However, more laser-equipped machines must be adopted on the industrial scale to achieve higher output, restricting this method to only laboratory-scaled production. Another well-established method of AgNP synthesis is using chemical processes involving the reduction reaction of silver ions into AgNP directly. Although this process is simple and straightforward, this method employs chemical-reducing agents that are hazardous and toxic in nature. For example, N, N-dimethylformamide (DMF) is a common and widely used reducing agent that is reported to cause damage to the liver and digestive system (EPA, 2023). To mitigate this, greener, eco-friendly, and low-energy consumption methods are being explored to synthesize AgNP for large-scale production, which is currently offered by the green synthesis method using suitable bioresources.

Plants are one of the most accessible bioresource materials that can be used as a bio-reducing agent to synthesize AgNP. The abundance of plants and their diverse types makes the potential for utilization near limitless. AgNP can be produced through a plant-mediated green synthesis technique after being reduced by the phenolic and flavonoid compounds present in the plant extracts. A fundamental study found that different plant-derived polyphenolic and flavonoid compounds have anticarcinogenic, immune-stimulating, anti-allergic, and anti-viral effects (Rice-evans et al., 1995). Hence, these properties are inherited by the usage and application of the plant for specific remedies to treat illnesses. Compared to other plants, *F. deltoidea* has been extensively studied for its antinociceptive (Sulaiman et al., 2008), anti-inflammatory (Abdullah et al., 2009), antioxidant (Bunawan et al., 2014), and anti-proliferative activities (Abolmaesoomi et al., 2019). The abundance of phytochemical contents influences these effects, thus making *F. deltoidea* a valuable plant to be integrated into the plant-mediated AgNP synthesis system.

Antibacterial-resistant bacteria have been widely acknowledged as problematic with the current dependency on antibiotics to treat illnesses. Since bacteria were overexposed to antibiotics, they became resistant, which resulted in reduced cellular absorption and increased efflux of drugs, their blockage by covalent modification, and the development of resistance genes that substitute for antibiotic-targeted substrate (Yan et al., 2022). *Escherichia coli*, a Gram-negative bacteria located in the gut of humans, has been considered harmless. However, studies found that pathogenic *E. coli* is resistant to first-line antibiotics (Longhi et al., 2022). Furthermore, commonly analyzed *Staphylococcus aureus* has been categorized into methicillin-resistant *S. aureus* (MRSA) due to the high cases of antibiotic-resistant *S. aureus* found in the healthcare system.

Furthermore, newer strains of MRSA have been reported to be resistant to glycopeptide antibiotics, which increases the difficulty in treating infectious wounds (Ahmed and Baptiste, 2018). A commensal lipophilic Gram-positive bacterium, *Cutibacterium acnes* is considered an aerotolerant anaerobe because it possesses enzyme systems that can detoxify oxygen, allowing for growth on the surface of the skin (Mayslich et al., 2021). Although known for maintaining healthy skin, *C. acnes* is considered an opportunistic bacterium due to its involvement in developing a skin disorder widely common in teenagers, which is *acne vulgaris* (Mayslich et al., 2021). The increasing use of cosmetic products to treat *acne vulgaris* has posed a threat to the increased resistance of *C. acnes* against commonly used antibacterial agents and antibiotics. It is reported that acne-resistant antibiotics have increased, ranging from <5% in Columbia to 100% in China (Karadag et al., 2021). As a result of the worrisome rise in bacterial resistance to

antibiotics, researchers are exploring novel antibacterial agents to manage bacterial resistance and treat various illnesses and bacterial infections. Hence, applying AgNP as an alternative form of antibiotic and antibacterial agent opens new possibilities to control these types of bacteria.

Concerns arise about the effects of the overuse of silver-based products on the environment and health. AgNP is known to possess a wide range of qualities that might be used in the biomedical field; nevertheless, without a thorough analysis of how AgNP would affect human biology, various health problems could occur. For example, uncontrolled silver release from silver-based products may form an aggregation of silver particles on the skin, thus resulting in skin diseases such as argyria or *argyrosis*, a condition for patients due to skin discoloration (Almurayshid, et al., 2020). Besides contact with the skin, humans can be exposed to AgNP by inhalation (Jaswal and Gupta, 2021), in which large AgNP can be exhaled out, while smaller AgNP will reach different organs via the bloodstream (Bamal et al., 2021). A study found that exposure to a high concentration of AgNP in mice causes significant brain injury (Rahman et al., 2009). At the cellular level, it was reported that the cytotoxicity effects of AgNP are at the same inhibitory range, at 10 ug/ml, which showed that AgNP has no selective effects against different cells (Vazquez-Muñoz et al., 2017).

Various cytotoxicity analyses and techniques can analyze such biocompatibility issues. One widely used biocompatibility assay is the colorimetric cell viability assay known as the 3-[4,5-Dimethylthiazol-2-yl]-2,5 diphenyl tetrazolium bromide (MTT) assay. In order to detect mitochondrial activity, the test relies on live cells transforming the MTT chemical into formazan crystals (Kamiloglu et al., 2020). The formation of the purple-colored crystals can be quantified spectroscopically at 570 nm. Because of this, viable and dead cells can be easily distinguished, thus making this assay a quick and easy method to analyze the biocompatibility of test samples against human cells. Although human studies on prolonged exposure to high doses of AgNP have not been extensively studied or reported, biocompatibility issues of AgNP as an antibacterial agent must be addressed so that safer AgNP-based products can be made and applied. This study investigated the use of local *F. deltoidea* (Mas Cotek) plant leaf aqueous extract by determining its phenolic and flavonoids contents as well as the subsequent AgNP formation for its characteristics and application as a biocompatible topical antibacterial agent against Gram positive, Gram negative and acne-causing bacteria.

METHODOLOGY

Sample preparation

Fresh *F. deltoidea* leaves were cut from the stems, washed, and thinly sliced before being extracted using a heat percolation method in a 60°C oven for 48 hours. After that, 100 mL of deionized water was added to 2 g of the leaves powder and extracted for 30 minutes at 100°C, making a mixture that was equivalent to 2% of the plant leaves. The mixture was then filtered, and the supernatant was stored at 4°C.

Total phenolic content (TPC)

The total phenolic content (TPC) of *F. deltoidea* extract was determined based on previous work (Din et al., 2021). Folin-Ciocalteu (FC) reagent and sodium carbonate solution were used in this test. The initial calibration curve for gallic acid (0.00, 0.01, 0.02, 0.04, 0.06, 0.08 and 0.10 mg/mL) was created by analyzing the standard calibration solution. Then, 1 mL of each gallic acid solution was added into a 15 mL centrifuge tube, followed by the addition of 0.5 mL FC reagent and 5 mL of deionized water. The mixture was left for 5 minutes at room temperature (24°C). After that, 10 mL of deionized water and 1.5 mL of sodium carbonate (20%) were added to the solution. The solution was placed in an oven at 40°C for 30 minutes. The standard solutions were analyzed using UV-visible spectroscopy at 750 nm. The same process was repeated using a solution containing plant leaf extract (2% concentration). The TPC value was calculated as the equation (1).

$$Total\ Phenolic\ Content, (GAE), = \frac{C_1 V}{M} \quad (1)$$

Where C_1 is the concentration gained from the calibration curve, V is the volume of plant extract (mL) while M is the mass of plant extract (g).

Total flavonoid content (TFC)

The reagents used in this test were aluminium chloride solution (10%), sodium hydroxide solution (1 M), and sodium nitrate solution (95%). To prepare a stock solution of 5 mg/mL of quercetin, 0.05 g of quercetin was dissolved in 100 mL of deionized water. From the stock quercetin solution, a series of concentrations, which were 0.02 mg/ml, 0.04 mg/ml, 0.06 mg/ml, 0.08 mg/ml, and 0.10 mg/ml were prepared. Accurately, 1 mL of the prepared standard solution was added with 0.3 mL of sodium nitrite solution, and 4 mL of deionized water was placed in a centrifuge tube, which was left at room temperature for 5 minutes. After that, 0.3 mL of aluminium chloride solution and 2 mL of sodium hydroxide 1 mM solution were added. Deionized water was added to the mixture one more time until a total amount of 10 mL was attained. The solution was then placed in an oven for 30 minutes at 40°C. After measuring each solution with a UV-visible spectrophotometer (Jenway 7200 Visible Spectrophotometer) at 510 nm, the calibration curve was then produced. The linear equation derived from the quercetin standard calibration curve was then used to calculate the TFC, and the TFC value was calculated as in equation (2).

$$Total\ Flavonoid\ Content, (QE), = \frac{C_1 V}{M} \quad (2)$$

Where, C_1 is the concentration gained from the calibration curve, V is the volume of plant extract (mL), and M is the mass of plant extract (g).

Biosynthesis of AgNP

F. deltoidea solutions were prepared with different concentrations (2%, 0.1%, 0.5%, 1.0%, 5.0%, and 10.0%) for the

optimization of AgNP synthesis. All the prepared plant extract concentrations were subjected to an optimization study to determine the parameters which yield the highest amount of AgNP. Initially, 1 mM of silver nitrate ($AgNO_3$) solution was prepared. Then, 10 ml of the $AgNO_3$ solution was added into a universal bottle along with 5 ml of each plant extract solution and left at room temperature (24°C) for 1 hour. The absorbance reading was recorded in the range of 450 nm to 850 nm using a UV-visible spectrophotometer (Jenway 7200 Visible Spectrophotometer) to determine the formation of AgNP. After the optimal concentration had been determined, the effect of different reaction volumes and reaction times was carried out. The different volumes of the extract (1 – 10 mL) with the optimal concentration were added to the prepared $AgNO_3$ solution. The color changes were observed, and the UV-vis spectrum was recorded. The optimal temperature was determined by subjecting the previous optimal condition to different synthesis temperatures (room temperature (24°C), 30°C, 40°C, 50°C, 60°C, 70°C and 80°C). The green synthesis of AgNP was done by eliminating the use of chemical-reducing agents in the synthesis method, which are known to be harmful and hazardous. Figure 1 illustrates the biosynthesis process of AgNP using plant extract as a green synthesis approach.

Figure 1. Biosynthesis process of AgNP using *F. deltoidea* plant leaves extract.

Characterization techniques

The UV-visible spectroscopy was used to determine the optimal yield of the AgNP in the optimization study. The surface plasmon resonance (SPR) of the AgNP was measured for AgNP colloidal solution using a Jenway 7200 Visible spectrophotometer with a quartz cuvette in the wavelength range from 350 nm to 750 nm. The peaks produced by this technique may also be used to find the approximate sizes of the biosynthesized AgNP in which the lower shifted wavelengths imply smaller AgNP sizes, whereas wider wavelengths indicate bigger AgNP sizes (Husain et al., 2023). The plant extract (FD-Extract) and biosynthesized colloidal (FDAgNP) were characterized using Fourier transform infrared spectroscopy (Perkin Elmer FTIR 1600) at the wavenumber range of 4000 - 450 cm^{-1}. The samples were initially mixed and ground thoroughly with KBr and transformed into small discs by a press machine. The pressed sample disc was removed and placed in the sample holder of the FTIR machine. Prior to the X-ray diffraction

analysis (XRD), the colloidal AgNP was centrifuged for 1 hour at 40°C and 10,000 rpm. The pellet was dried in an oven at 80°C for 24 hours after the supernatant was drained. The pellet was maintained in a desiccator after being crushed and processed in a mortar and pestle. The AgNP powdered sample was sonicated for 30 minutes in distilled water before drying on clean filter paper. A Rigaku SmartLab X-ray diffractometer was used in the XRD analysis at λ= 1.5418 at 40 kV and 30 mA in the 2θ = 3°-100° range at a scanning rate of 0.02°/second. The morphology and approximate sizes of the biosynthesized AgNP were analyzed using a transmission electron microscope (TEM). Approximately 10 µl of the sample was transferred into a thin carbon film which was then supported by the copper grid. The grid was put in a sample container once the forceps were lifted. The TEM images were obtained using JEOL model JEM-ARM200-F.

Antibacterial assay

The antibacterial study was carried out by initial preparation of several media and continued with disc diffusion technique (DDT) against Gram-negative *E. coli* ATCC 11229, Gram-positive *S. aureus* ATCC 6538 and anaerobic *C. acnes* ATCC 11827 bacteria. Three to four colonies of *S. aureus* and *E. coli* were inoculated on agar plates and resuspended in a separate saline solution for DDT. The solution turbidity was corrected using 0.5 McFarland standard (1.5×10^8 CFU (Colony Forming Unit)/mL) and streaked across the media surface. Finally, 300 µL of the colloidal AgNP samples were carefully pipetted into a sterilized susceptibility disc, and they were allowed to dry on the disc. The discs were placed on the surface of growth media streaked with the bacteria and left to incubate at 37°C overnight. The halo zone was measured by the observed area of the inhibition zone, which appeared at the edge of the tested samples. The same technique was carried out for *C. acnes* bacteria; however, the turbidity of the bacterial suspension was adjusted to OD600 of 0.14 (1×10^8 CFU/mL) using phosphate-buffered saline (PBS) and cultured in an Anaerobe Container System (GasPak EZ) at 37°C for 4 to 7 days.

In vitro cytotoxicity study of biosynthesized AgNP

The MTT test was used to evaluate the in vitro cell viability of HSF 1184 cells. After being exposed to the commercialized AgNP (CAgNP) and biosynthesized AgNP (BAgNP), the viability of the cell was assessed using a colorimetric technique. To prevent overexposure to light, 10 mg of MTT was placed in a centrifuge tube and covered with aluminium foil. The mixture was then dissolved with 2 mL of PBS. A 0.22 m sterile syringe filter and syringe were used to filter the mixture before placing it in another centrifuge tube. Next, 20 mL of cDMEM (Dulbecco's modified eagle medium) were vortexed. On the 24-well plate, 900 µL of the previous media was removed from each well. Then, 770 µL MTT mixture was pipetted into the wells. For the reactions to occur, the plate was wrapped in aluminium foil and placed in a CO_2 incubator for around three hours. The cells were then examined using an inverted light microscope, and the connected camera was used to take a photomicrograph of the cells. Later, 350 µL of dimethylsulfoxide (DMSO) was added as a buffer after 100 L of the medium was pipetted out. The pipette was used to homogenize the mixture. Next, 200 µL of the plate's reacted solution was poured into a 96-well plate. Finally, an ELISA microplate reader (Promega Glomax) was used to measure the absorbance (OD) of each well at 540 nm.

Statistical analysis was done by using GraphPad Prism software with two-way ANOVA analysis to quantify the significance of the data between the samples and test organisms.

RESULTS AND DISCUSSION

Plant analysis

The TPC value of *F. deltoidea* plant leaf extract was determined as 24.37 ± 0.57 mg/g, and the TFC value was 1118.91 ± 8.55 mg/g. Due to many circumstances, including the plant's original environment and the extraction solvent utilized, such as the use of methanol and ethanol during the extract production, these results were different to those of earlier research (Kumari and Dhanalekshmi, 2017). A polar solvent has a superior efficiency of solvation due to the stronger interaction of hydrogen bonds between the polar sites of the antioxidants. It has been established that different extraction solvents can alter the TPC and TFC values due to the solvent's polarity (Thouri et al., 2017). However, in order to retain the green synthesis approach in this work, which may be accomplished without the use of organic solvents, the leaf extraction was carried out using water (aqueous extract).

Optimization of AgNP synthesis

The synthesis of AgNP was optimized in accordance with its various concentrations, temperatures, volumes, reaction times, and pH solution. Figure 2 shows the UV-visible spectra and the absorbance values for each optimization parameter. It was discovered that the optimal concentration for AgNP production at this stage was 5% of the plant leaf extract, where the maximum SPR peak was observed. It is also observed that the SPR of AgNP was red shifted at ~450 nm with the addition of higher concentrations of plant extract, indicating a larger formation of AgNP size (Rajput et al., 2020). Figure 2(b) shows the effects of different temperatures on AgNP synthesis, which exhibits a higher SPR peak with the increase in temperature. A higher temperature enhances the reaction rate because the Ag^+ ions are consumed during the production of the nuclei, which halts the process of secondary growth on the surface of the pre-formed nuclei (Song and Kim, 2009). In return, higher temperature results in higher purity and smaller sized nanoparticles (Salunke et al., 2014). The optimal volume of the plant extract was determined to be 0.6 ml, which produces the highest peak observed in the visible spectra. Interestingly, lower volumes of plant extract produced visible spectra at lower wavelength, indicating smaller sized AgNP. The volume of plant extract correlates with the concentration of phytochemicals found in the plant extract, whereby the lesser volume of plant extract has fewer phytochemical contents. It is well established that the phytochemical compounds are responsible for the reduction of Ag^+ into AgNP. A study showed that higher concentrations of phytochemicals increase the size of AgNP (Johnson and Prabu, 2015).

(i) (ii)

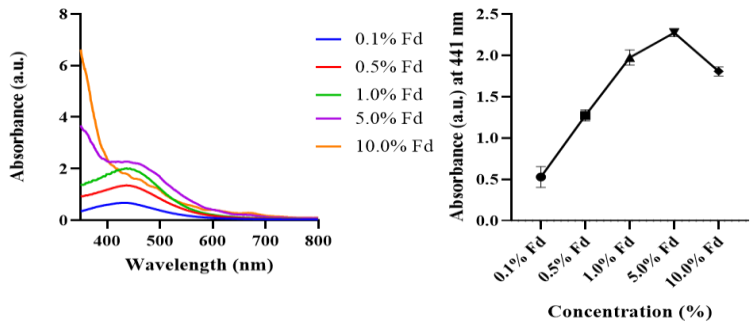

(a)

(i) (ii)

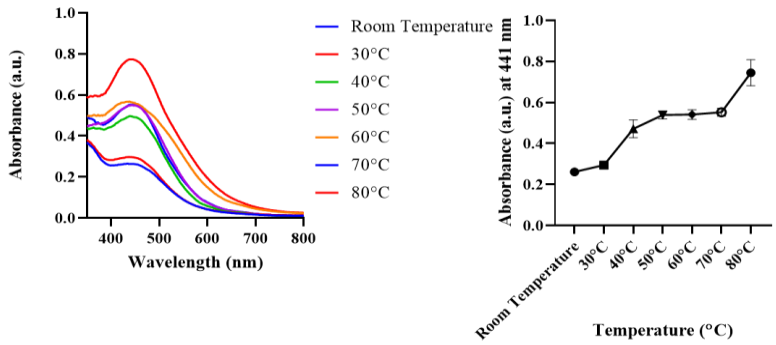

(b)

(i) (ii)

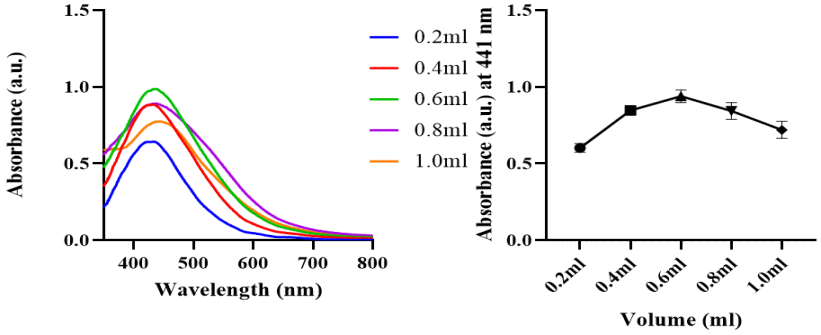

(c)

(i) (ii)

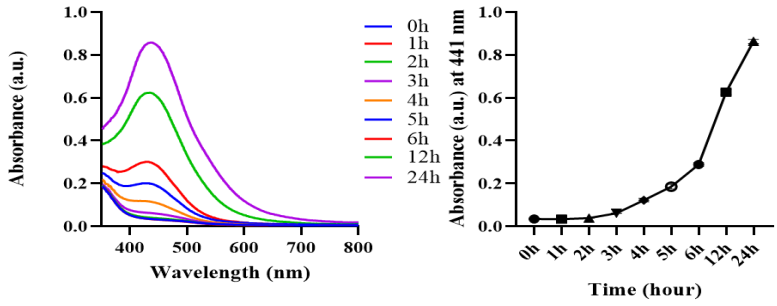

(d)

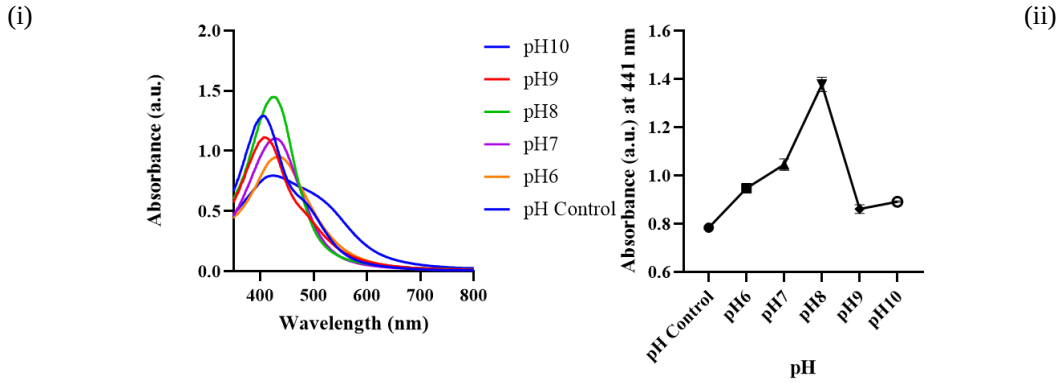

(e)

Figure 2. (i) Visible spectra of AgNP synthesized at different (a) plant extract concentrations, (b) temperatures, (c) volumes, (d) time, and (e) pH and (ii) the absorption values of the AgNP at 441 nm with their respective parameters.

The high intensity SPR band at 441 nm rises with time, and it was decided that 24 hours was the best time for a high yield of AgNP. This indicates that the reaction time is required for the complete reduction of Ag to be completely reduced to AgNP. Studies have shown that reaction times influence the yield of AgNP for the complete reduction process (Din et al., 2022; Rajput et al., 2020). The pH values greatly influence the yield of AgNP. High AgNP yield was observed at pH 8, which is consistent with the previous study indicating that the AgNP synthesis produced higher yields under slightly alkaline conditions (Elemike et al., 2017). The high OH^- content of the extracts is thought to optimize the electrostatic and electrosteric repulsion, which improves AgNP stability (Elemike et al., 2017). In this study, it was determined that the optimal synthesis of the AgNP using *F. deltoidea* plant leaf extract was at 0.6 ml of plant leaf extract with a concentration of 5%, at 80°C of synthesis temperature with a pH value of 8 for 24 hours.

Characterization

Structural properties

The functional groups involved in the synthesis of AgNP can be examined using FTIR spectroscopic technique. The AgNP was stabilized by phytochemicals serving as capping agents, and FTIR analysis was able to confirm multiple functional groups in the samples. Figure 3 shows the comparison between FTIR spectra of the plant extract (FD-Extract), and the biosynthesized colloidal AgNP (FDAgNP). Based on Figure 3, the sharp peak in the FTIR spectra at 1640 cm^{-1} represents the C=O (carbonyl) group and the peak at 3320 cm^{-1} was attributed to the amines and hydroxyl functional groups. These functional groups are found prominently due to the presence of phytochemicals in the plant extract. Phytochemicals are plant metabolites that are thought to have a significant role in the biological defenses against pathogens (Cory and Hoover, 2006) and oxidative stress (Misbah et al., 2013). Recent research has revealed that the leaf extract of the *F. deltoidea* plant contains a number of phytochemicals, including gallic acid, P-coumaric acid, chlorogenic acid, and luteolin-7-glucoside with the highest concentration of gallic acid is found in the leaves of *F. deltoidea* compared to other organs of the plant (Din et al., 2022). Gallic acid is a compound found in plants which contains hydroxyl and carbonyl functional groups (Goldberg and Rokem, 2009), P-coumaric acid, luteolin-7-

glucoside and chlorogenic acid contains an abundance of hydroxyl groups (National Center for Biotechnology Information, 2023) which strengthened the results obtained from the FTIR spectra, showing the high peak obtained at the 3320 cm^{-1} regions.

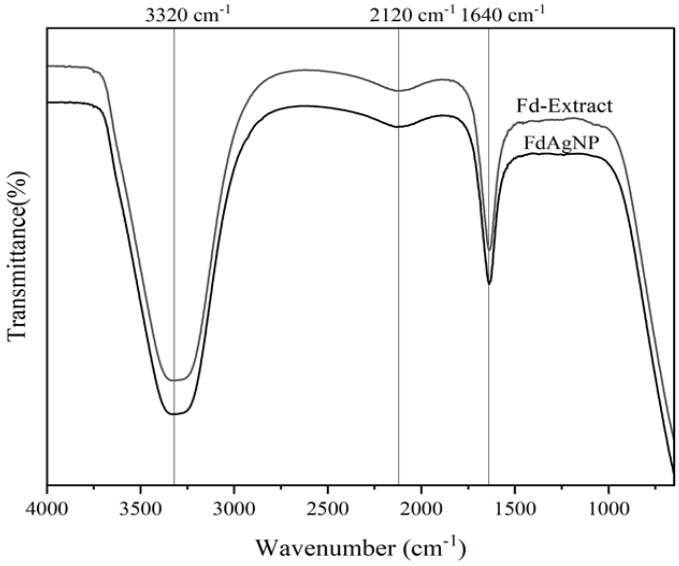

Figure 3. FTIR spectra of the plant extract (FD-Extract) and biosynthesized colloidal (FDAgNP).

The XRD analysis was performed to examine the crystalline nature of the biosynthesized AgNP (BAgNP). The colloidal AgNP was centrifuged and dried to obtain powdered AgNP. Moreover, the applied heat was able to evaporate the solution and, in return, gave the sample powder with higher purity. Figure 4 shows the XRD pattern of the biosynthesized AgNP.

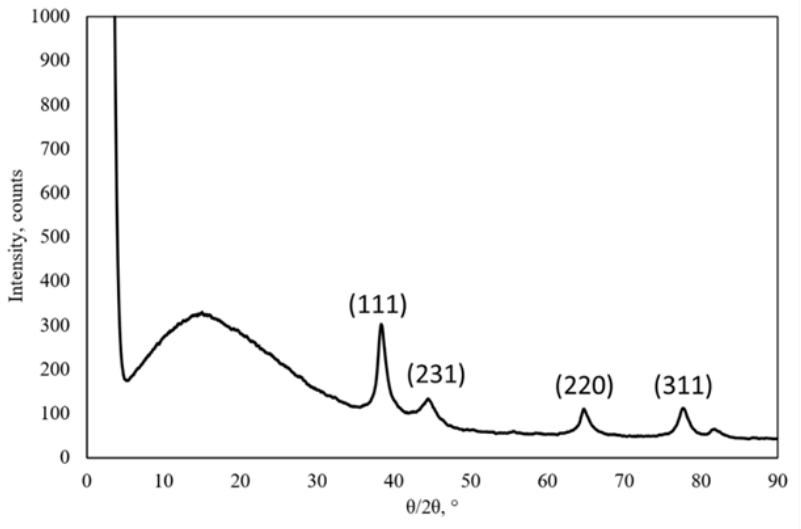

Figure 4. XRD pattern of the biosynthesized AgNP.

The crystalline nature of the biosynthesized AgNP is shown in Figure 4, where the peaks obtained at 38°, 46°, 64° and 76° correspond to the lattice parameters (111), (231), (220), and (311), which are closely connected with JCPDS (Card No. 04–0783) for silver (Debnath et al., 2020). This shows that the crystalline structure is face-centered cubic

of metallic silver, which is similar to other studies (Çalhan and GÜndoĞan, 2020; Din et al., 2022). In addition to the metallic silver phase, the diffractogram displayed a few additional unassigned peaks. The unassigned peak, which was recorded at the region of 10° to 30°, corresponds to the amorphous state of the plant extract within the sample (Wan Mat Khalir et al., 2020). The bioorganic crystallized phase of the biosynthesized AgNP, which serves as the capping agent, is responsible for the formation of these additional crystalline phases, corresponding to the organic moiety (Asimuddin et al., 2020). This result also validates the results from the FTIR analysis (Figure 3) for the functional groups present in the sample.

Morphological properties

TEM was utilized to investigate the morphology of the biosynthesized AgNP due to its nano-dimension and characteristics. Furthermore, the approximation of the particle size was determined by ImageJ software by calibrating the image obtained from the TEM result. Figure 5 shows the TEM images at 100× and 200× magnifications. The morphology of the AgNP was observed to be spherical in shape, with approximate sizes ranging from 10 nm to 50 nm. Due to the numerous phytochemicals contained in the plant extract, which serve as the reducing agent for the AgNP synthesis, the varying sizes demonstrate that the nucleation rates of AgNP are not completely uniform. This result correlates to the FTIR analysis, which shows different functional groups from the diverse compounds in the plant extract. Moreover, the particle sizes which was analyzed are important in determining the antibacterial efficacy of the AgNP, where a smaller sized AgNP has a higher antibacterial effect (Quintero-Quiroz et al., 2019).

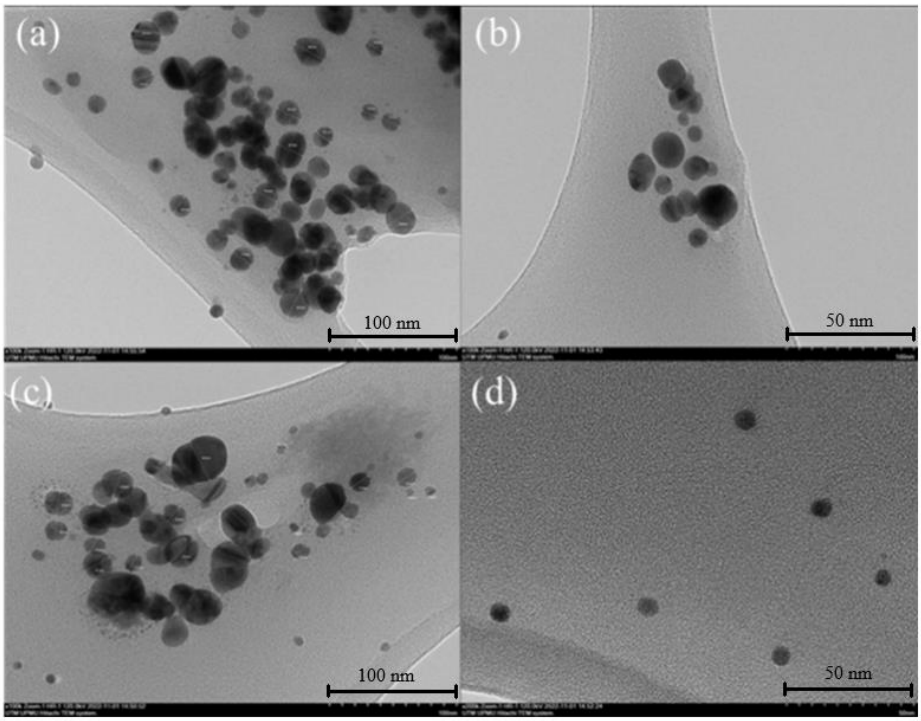

Figure 5. TEM images at 100× magnification (a), (c), and 200× (b), (d).

Antibacterial analysis

The biosynthesized AgNP was evaluated for its antibacterial effect by culturing the selected bacteria according to its growth medium. Bacteria *S. aureus* and *E. coli* were grown on Mueller Hinton agar (MHA) media, and *C. acnes* was grown on reinforced clostridial agar (RCA). The analysis was done consecutively with distilled water and plant extract as negative control samples, whereas colloidal AgNP (FDAgNP) was used as a positive control. Two types of antibiotic discs were used in this analysis as positive control samples. MHA media was loaded with cefoxitin disc, whereas the RCA media was loaded with ampicillin, as shown in Figure 6. Figure 6 and Table 1 revealed the antibacterial effect of the test samples containing AgNP. The antibacterial activity of the AgNP might be due to the reactive oxygen species (ROS) interaction of the bacterial cellular membrane (Samuggam et al., 2021). A study has shown that the concentration of ROS influences the growth of bacteria by inducing oxidative stress, which damages cellular membranes, proteins, DNA/RNA, and lipids (Samuggam et al., 2021). Interestingly, the plant leaf extract exhibits antibacterial effects against *S. aureus* and *C. acnes* measured at 4.6 ± 0.3 mm and 11 ± 1.6 mm, respectively. The antibacterial effects of the extract are dependent on various parameters such as the phytochemicals found in the plant extract, the condition of the plant extract and the bacterial morphology. The pH of *F. deltoidea* was measured at 5, which is slightly lower in accordance with previous research that examined various pH values of *C. acnes* growth and found that it has an antibacterial effect at the pH range of 2.5 to 5.5. (Valle-González et al., 2020).

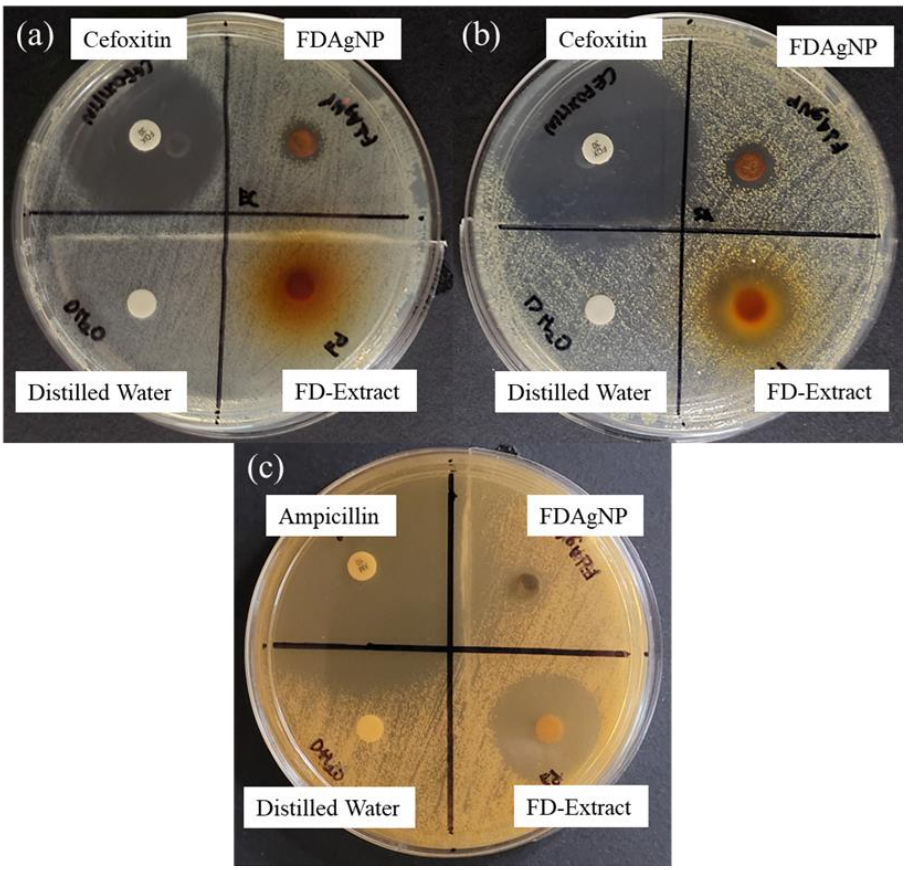

Figure 6: DDT images of tested samples against (a) *E. coli*, (b) *S. aureus* and (c) *C. acnes*.

Table 1. The inhibition zone values measured according to the DDT analysis for the test bacteria.

Sample	Inhibition zone (mm)		
	E. coli	*S. aureus*	*C. acnes*
FDAgNP	2.3 ± 0.1	3.2 ± 0.2	3 ± 0.8
Cefoxitin	13 ± 0.5	15 ± 0.3	-
Ampicillin	-	-	25 ± 2.1
Plant Extract	None	4.6 ± 0.3	11 ± 1.6
Distilled water	None	None	None

Antibacterial analysis of biosynthesized AgNP against skin bacteria

The DDT analysis of 2 mg/ml BAgNP and CAgNP against skin bacteria *C. acnes* shows somewhat similar inhibition zones produced and measured, as shown in Figure 7 and Table 2. The mechanism and action of AgNP antibacterial have been discussed due to the ROS, which induced the oxidative stress response of the cellular environment.

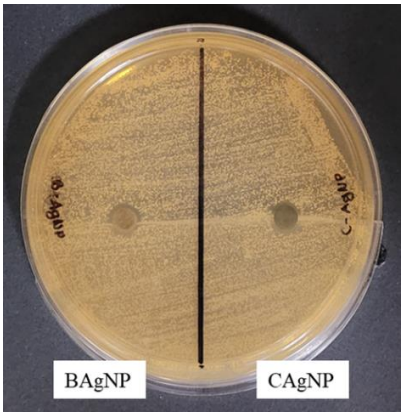

Figure 7. DDT image of *C. acnes* treated with BAgNP and CAgNP.

Table 2. Inhibition zone measured by the DDT analysis of *C. acnes* with different types of AgNP

Sample	*C. acnes* inhibition zone (mm)
BAgNP	3 ± 1.4
CAgNP	2 ± 1.4

The higher BAgNP effect is due to the various bioactive compounds found in the plant extract, which act as capping agents, resulting in the high number of antioxidants that may be associated with ROS over-production, which is dependent on concentration and incubation time (Osseni, 2000). Hence, higher antibacterial effects and oxidative stress response are induced towards the bacteria compared to CAgNP. *C. acnes* is well recognized for being an anaerobic bacterium, which cannot grow on a solid medium when ambient oxygen is present, and thus, the ROS over-production within the cell constitutes the higher inhibition zones and lower growth observed from the DDT plate.

Cytocompatibility study via MTT assay

As shown in Figure 8, it can be observed that BAgNP has higher cytotoxicity due to the lower inhibitory concentration (IC_{50}). IC_{50} is a measurement of the cytotoxicity of a drug which is tested against whole cells and indicates the amount of a material needed to inhibit a biological process (Aykul and Martinez-Hackert, 2016). In this case, the value was

observed at 50% of the inhibitory growth condition, which is at 0.25 mg/ml of BAgNP that inhibits the biological process and causes cell apoptosis due to the decreased in the percentage of cell viability compared to the higher concentrations of CAgNP, at 1.0 mg/ml. Hence, this data shows that a lower concentration of BAgNP causes lower cell viability and, thus, higher cytotoxicity effects against HSF 1184.

Comparing cytotoxicity of BAgNP, CAgNP had less cytotoxicity effects towards the cell samples. This demonstrates the capability of the biosynthesized AgNP to restrict cellular survival and proliferation and shows that AgNP affects both bacterial and human cells in a much larger spectrum. On the other hand, using biosynthesized AgNP for human application is technically possible, with cautious administration and regulated dose. From an industrial standpoint, upscaling the synthesis of BAgNP will prove to be cost-effective due to the dilution of raw BAgNP needed to produce and manufacture biocompatible consumer products. This is because a lesser concentration of BAgNP is needed without exhibiting cytotoxicity effects while promoting antibacterial benefits.

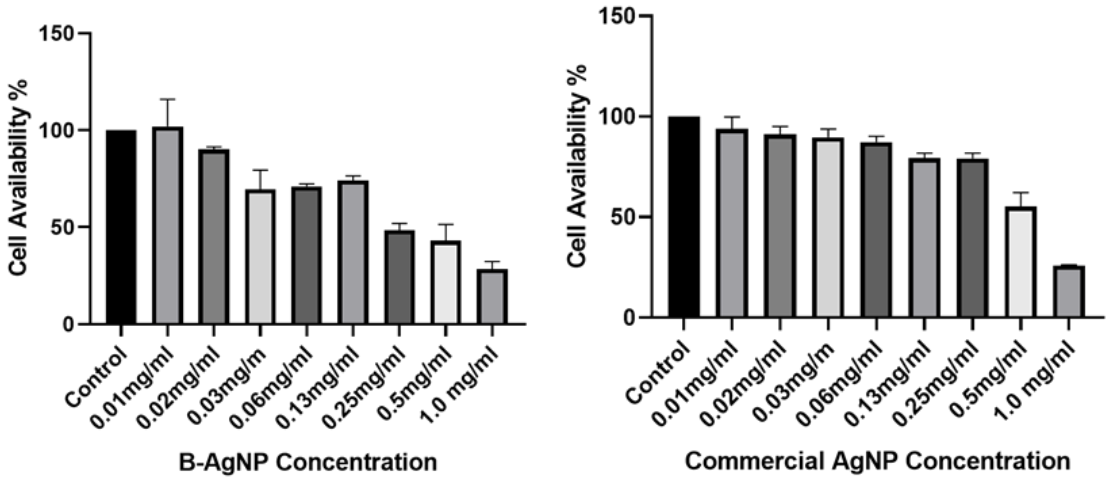

Figure 8. Cytotoxicity analysis for BAgNP and CAgNP against normal human fibroblast cells in vitro.

CONCLUSION

This study demonstrated that the AgNP can be synthesized using bioresource, which is plant leaves aqueous extract of *F. deltoidea* (Mas Cotek) due to the high antioxidant activity found in the plant leaf extract. The aqueous plant extract could reduce Ag^{+} (from $AgNO_3$) to Ag^{0} (AgNP) as presented in the UV-vis spectra around 450 nm due to the SPR of Ag^{0}. The particles of the biosynthesized AgNP are spherical, with sizes ranging from 10 nm to 50 nm. FTIR results indicate the functional groups responsible for the reduction process, which are mainly carbonyl and hydroxyl groups that come from the plant extract. Moreover, the crystallization phase was determined to be Ag element due to the similarity of lattice parameters. The biosynthesized AgNP has high antibacterial activity against a wide spectrum of bacteria, including Gram positive and Gram-negative bacteria as well as anaerobic bacteria. Furthermore, the biosynthesized AgNP has mild cytotoxicity against normal human cells. This study has successfully demonstrated the ability of the local plant herb of *F. deltoidea* aqueous extract in the biosynthesis of AgNP, and the biosynthesized AgNP can be used as an excellent antibacterial agent with low toxicity, which is suitable as an alternative

dermatological antibacterial agent.

ACKNOWLEDGMENTS

The authors would like to express gratitude to the Ministry of Higher Education and Universiti Teknologi Malaysia for funding and supporting this research project under the Fundamental Research Grant Scheme (FRGS/1/2020/STG04/UTM/02/3) with Vot No: 5F291.

AUTHOR CONTRIBUTIONS

Ibrahirul Qamil Ismail: investigation, methodology framework, data analysis, and writing; **Nik Ahmad Nizam Nik Malek**: conceptualization, methodology, proofreading and reviewing; **Nor Suriani Sani:** methodology; **Muhammad Hariz Asraf:** proofreading and methodology; **Shahrulnizahana Mohammad Din**: conceptualization and methodology.

FUNDINGS

Fundamental Research Grant Scheme (FRGS/1/2020/STG04/UTM/02/3) with Vot No: 5F291.

COMPETING INTEREST

The authors would like to declare that there are no conflicts of interest.

COMPLIANCE WITH ETHICAL STANDARDS

Not applicable.

SUPPLEMENTARY MATERIAL

Not applicable.

REFERENCES

Abdullah, Z., Hussain, K., Ismail, Z., & Ali, R. M. (2009). Anti-inflammatory activity of standardized extracts of leaves of three varieties of *Ficus deltoidea.* International Journal of Pharmaceutical and Clinical Research, 1(3), 100-105.

Abolmaesoomi, M., Aziz, A. A., Junit, S. M., & Ali, J. M. (2019). *Ficus deltoidea*: Effects of solvent polarity on antioxidant and anti-proliferative activities in breast and colon cancer cells. European Journal of Integrative Medicine, 28, 57-67.

Ahmed, M. O., & Baptiste, K. E. (2018). Vancomycin-resistant enterococci: a review of antimicrobial resistance mechanisms and perspectives of human and animal health. Microbial Drug Resistance, 24(5), 590-606.

Almurayshid, A., Park, S., & Oh, S. H. (2020). Effective laser treatment options for argyria: Review of literatures. Journal of Cosmetic Dermatology, 19(8), 1877-1882.

Asimuddin, M., Shaik, M. R., Adil, S. F., Siddiqui, M. R. H., Alwarthan, A., Jamil, K., & Khan, M. (2020). *Azadirachta indica* based biosynthesis of silver nanoparticles and evaluation of their antibacterial and cytotoxic effects. Journal of King Saud University-Science, 32(1), 648-656.

Aykul, S., & Martinez-Hackert, E. (2016). Determination of half-maximal inhibitory concentration using biosensor-based protein interaction analysis. Analytical Biochemistry, 508, 97-103.

Bamal, D., Singh, A., Chaudhary, G., Kumar, M., Singh, M., Rani, N., & Sehrawat, A. R. (2021). Silver nanoparticles biosynthesis, characterization, antimicrobial activities, applications, cytotoxicity, and safety issues: An updated review. Nanomaterials, 11(8), 2086.

Bunawan, H., Amin, N. M., Bunawan, S. N., Baharum, S. N., & Mohd Noor, N. (2014). *Ficus deltoidea* Jack: a review on its phytochemical and pharmacological importance. Evidence-Based Complementary and Alternative Medicine, 2014, 902734.

Çalhan, S. D., & GÜndoĞan, M. (2020). Biosynthesis of silver nanoparticles using *Onosma sericeum* Wild. and evaluation of their catalytic properties and antibacterial and cytotoxic activity. Turkish Journal of Chemistry, 44(6), 1587-1600.

Cory, J. S., & Hoover, K. (2006). Plant-mediated effects in insect–pathogen interactions. Trends in ecology & evolution, 21(5), 278-286.

Debnath, B., Sarkar, S., & Das, R. (2020). Effects of saponin capped triangular silver nanocrystals on the germination of *Pisum sativum*, *Cicer arietinum*, *Vigna radiata* seeds & their subsequent growth study. IET Nanobiotechnology, 14(1), 25-32.

Din, S. M., Malek, N. A. N. N., Shamsuddin, M., & Matmin, J. (2021). Effect of plant organs of *Ficus deltoidea* in the synthesis of silver nanoparticles. Malaysian Journal of Analytical Sciences, 25(5), 716-727.

Din, S. M., Malek, N. A. N. N., Shamsuddin, M., Matmin, J., Hadi, A. A., & Asraf, M. H. (2022). Antibacterial silver nanoparticles using different organs of *Ficus deltoidea* Jack var. kunstleri (King) Corner. Biocatalysis and Agricultural Biotechnology, 44, 102473.

Elemike, E. E., Onwudiwe, D. C., Arijeh, O., & Nwankwo, H. U. (2017). Plant-mediated biosynthesis of silver nanoparticles by leaf extracts of *Lasienthra africanum* and a study of the influence of kinetic parameters. Bulletin of Materials Science, 40, 129-137.

EPA. (2023). Chemical Assessment Summary of N,N-Dimethylformamide. Retrieved from https://cfpub.epa.gov/.

Goldberg, I., & Rokem, J. S. (2009). Organic and fatty acid production, microbial. Encyclopedia of microbiology, 421-442.

Husain, S., Nandi, A., Simnani, F. Z., Saha, U., Ghosh, A., Sinha, & Verma, S. K. (2023). Emerging trends in advanced translational applications of silver nanoparticles: a progressing dawn of nanotechnology. Journal of Functional Biomaterials, 14(1), 47.

Jaswal, T., & Gupta, J. (2023). A review on the toxicity of silver nanoparticles on human health. Materials Today: Proceedings, 81, 859-863.

Johnson, I., & Prabu, H. J. (2015). Green synthesis and characterization of silver nanoparticles by leaf extracts of *Cycas circinalis*, *Ficus amplissima*, *Commelina benghalensis* and *Lippia nodiflora*. International Nano Letters, 5(1), 43-51.

Kaabipour, S., & Hemmati, S. (2021). A review on the green and sustainable synthesis of silver nanoparticles and one-dimensional silver nanostructures. Beilstein Journal of Nanotechnology, 12(1), 102-136.

Kamiloglu, S., Sari, G., Ozdal, T., & Capanoglu, E. (2020). Guidelines for cell viability assays. Food Frontiers, 1(3), 332-349.

Karadag, A. S., Aslan Kayıran, M., Wu, C. Y., Chen, W., & Parish, L. C. (2021). Antibiotic resistance in acne: changes, consequences and concerns. Journal of the European Academy of Dermatology and Venereology, 35(1), 73-78.

Kumari, U., & Dhanalekshmi, R. A. (2017). Evaluation of phytochemicals and antioxidant properties of leaves, fruits and stems of *Ficus deltoidea* plant extract. Scholars Res Lib, 8, 11-8.

Longhi, C., Maurizi, L., Conte, A. L., Marazzato, M., Comanducci, A., Nicoletti, M., & Zagaglia, C. (2022). Extraintestinal pathogenic *Escherichia coli*: Beta-lactam antibiotic and heavy metal resistance. Antibiotics, 11(3), 328.

Mayslich, C., Grange, P. A., & Dupin, N. (2021). *Cutibacterium acnes* as an opportunistic pathogen: An update of its virulence-associated factors. Microorganisms, 9(2), 303.

Misbah, H., Aziz, A. A., & Aminudin, N. (2013). Antidiabetic and antioxidant properties of *Ficus deltoidea* fruit extracts and fractions. BMC complementary and alternative medicine, 13, 1-12.

National Center for Biotechnology Information (NCBI)[Internet]. Bethesda (MD): National Library of Medicine (US), National Center for Biotechnology Information; 2023 – cited 2023 Apr 23. Available from: https://www.ncbi.nlm.nih.gov/

Osseni, R. A., Rat, P., Bogdan, A., Warnet, J. M., & Touitou, Y. (2000). Evidence of prooxidant and antioxidant action of melatonin on human liver cell line HepG2. Life Sciences, 68(4), 387-399., 1-12.

Quintero-Quiroz, C., Acevedo, N., Zapata-Giraldo, J., Botero, L. E., Quintero, J., Zárate-Triviño, D., ... & Pérez, V. Z. (2019). Optimization of silver nanoparticle synthesis by chemical reduction and evaluation of its antimicrobial and toxic activity. Biomaterials research, 23, 1-15.

Rahman, M. F., Wang, J., Patterson, T. A., Saini, U. T., Robinson, B. L., Newport, G. D., & Ali, S. F. (2009). Expression of genes related to oxidative stress in the mouse brain after exposure to silver-25 nanoparticles. Toxicology letters, 187(1), 15-21.

Rajput, S., Kumar, D., & Agrawal, V. (2020). Green synthesis of silver nanoparticles using Indian Belladonna extract and their potential antioxidant, anti-inflammatory, anticancer and larvicidal activities. Plant Cell Reports, 39, 921-939.

Rice-evans, C. A., Miller, N. J., Bolwell, P. G., Bramley, P. M., & Pridham, J. B. (1995). The relative antioxidant activities of plant-derived polyphenolic flavonoids. Free Radical Research, 22(4), 375-383.

Salunke, B. K., Shin, J., Sawant, S. S., Alkotaini, B., Lee, S., & Kim, B. S. (2014). Rapid biological synthesis of silver nanoparticles using *Kalopanax pictus* plant extract and their antimicrobial activity. Korean Journal of Chemical Engineering, 31, 2035-2040.

Samuggam, S., Chinni, S. V., Mutusamy, P., Gopinath, S. C., Anbu, P., Venugopal, V., & Enugutti, B. (2021). Green synthesis and characterization of silver nanoparticles using *Spondias mombin* extract and their antimicrobial activity against biofilm-producing bacteria. Molecules, 26(9), 2681.

Song, J. Y., & Kim, B. S. (2009). Rapid biological synthesis of silver nanoparticles using plant leaf extracts. Bioprocess and Biosystems Engineering, 32, 79-84.

Valle-González, E. R., Jackman, J. A., Yoon, B. K., Mokrzecka, N., & Cho, N. J. (2020). pH-dependent antibacterial activity of glycolic acid: implications for anti-acne formulations. Scientific Reports, 10(1), 7491.

Sulaiman, M. R., Hussain, M. K., Zakaria, Z. A., Somchit, M. N., Moin, S., Mohamad, A. S., & Israf, D. A. (2008). Evaluation of the antinociceptive activity of *Ficus deltoidea* aqueous extract. Fitoterapia, 79(7-8), 557-561.

Thouri, A., Chahdoura, H., El Arem, A., Omri Hichri, A., Ben Hassin, R., & Achour, L. (2017). Effect of solvents extraction on phytochemical components and biological activities of Tunisian date seeds (var. Korkobbi and Arechti). BMC Complementary and Alternative Medicine, 17(1), 1-10.

Vazquez-Muñoz, R., Borrego, B., Juárez-Moreno, K., García-García, M., Morales, J. D. M., Bogdanchikova, N., & Huerta-Saquero, A. (2017). Toxicity of silver nanoparticles in biological systems: does the complexity of biological systems matter?. Toxicology Letters, 276, 11-20.

Verma, S., Rao, B. T., Srivastava, A. P., Srivastava, D., Kaul, R., & Singh, B. (2017). A facile synthesis of broad plasmon wavelength tunable silver nanoparticles in citrate aqueous solutions by laser ablation and light irradiation. Colloids and Surfaces a: Physicochemical and Engineering Aspects, 527, 23-33.

Yan, L., Gopal, A., Kashif, S., Hazelton, P., Lan, M., Zhang, W., & Chen, X. (2022). Metal organic frameworks for antibacterial applications. Chemical Engineering Journal, 435, 134975.

Wan Mat Khalir, W. K. A., Shameli, K., Jazayeri, S. D., Othman, N. A., Che Jusoh, N. W., & Hassan, N. M. (2020). Biosynthesized silver nanoparticles by aqueous stem extract of *Entada spiralis* and screening of their biomedical activity. Frontiers in chemistry, 8, 620.